Communication: Vibrational spectroscopy of Au4 from high resolution photoelectron imaging

Zheng Yang, Iker Leon, and Lai-Sheng Wang

Citation: The Journal of Chemical Physics **139**, 021106 (2013); doi: 10.1063/1.4813503
View online: http://dx.doi.org/10.1063/1.4813503
View Table of Contents: http://scitation.aip.org/content/aip/journal/jcp/139/2?ver=pdfcov
Published by the AIP Publishing

Communication: Vibrational spectroscopy of Au_4 from high resolution photoelectron imaging

Zheng Yang, Iker Leon, and Lai-Sheng Wang[a)]
Department of Chemistry, Brown University, Providence, Rhode Island 02912, USA

(Received 30 May 2013; accepted 26 June 2013; published online 10 July 2013)

High resolution photoelectron spectroscopy of Au_4^- is reported using a new photoelectron imaging apparatus. A broad vibrational progression is resolved for the detachment transition from the ground electronic state of the Y-shaped Au_4^- to that of the Y-shaped Au_4 neutral (C_{2v}, $^1A_1$) in the ν_2 vibrational mode with a harmonic frequency of 171(7) cm^{-1} and an anharmonicity of ~0.5 cm^{-1}. In addition, two low frequency modes with weak Franck-Condon factors are observed: the υ_3 mode with a frequency of 97(7) cm^{-1} and the υ_6 mode with a frequency of 17(7) cm^{-1}. An accurate electron affinity of 2.7098(6) eV is obtained for the Y-shaped Au_4 neutral cluster. The current study shows that very low frequency vibrational modes can be resolved for size-selected clusters using high resolution photoelectron imaging, providing valuable additional experimental information for cluster structure determination. © *2013 AIP Publishing LLC*. [http://dx.doi.org/10.1063/1.4813503]

Recently we reported the first result from a newly developed high resolution photoelectron (PE) imaging apparatus on Au_2^-.[1] Vibrational peak widths as narrow as 3 cm^{-1} were resolved in the photoelectron images of Au_2^-. Photoelectron spectroscopy (PES) is a powerful technique for the study of size-selected atomic clusters, yielding electronic structure information which has been combined with theoretical calculations to obtain cluster structures. However, vibrational structures are usually not resolved in PES of size-selected clusters because of the limited spectral resolution. The imaging technique, originally developed for photodissociation,[2] has emerged as a high resolution PES method over the past decade, in particular, for slow electrons.[3,4] In addition to the high spectral resolution, PE imaging also yields photoelectron angular distributions. The high resolution capability of PE imaging should allow vibrational structures to be routinely obtained for size-selected clusters, providing valuable additional information for cluster structure determination. In this Communication, we report high resolution photoelectron imaging on the Au_4^- cluster. We resolved three vibrational modes for Au_4, including the very low frequency υ_6 mode with an observed frequency of 17 cm^{-1}. The vibrational information is used to compare with calculated frequencies, yielding unequivocal structural information.

The Au_4^- cluster has been investigated extensively.[5–13] Structures of Au_n^- ($n < 13$) were studied by ion mobility and density functional theory (DFT).[9] A zig-zag chain, a Y-shape (C_{2v}), and a rhombus (D_{2h}) structure were found to be close in energy, but comparison between experimental and computed cross sections showed that the observed Au_4^- was the Y-shaped structure (an Au atom bonded to the apex of a Au_3 triangle). A subsequent PES and DFT study also found that the Y-shaped Au_4^- was in agreement with the observed adiabatic (ADE) and vertical (VDE) electron detachment energies.[11] More recently, Au_4^- and Au_4 were studied at various levels of theory, and at the most sophisticated level of theory the Y-shaped isomer was confirmed to be the global minimum of Au_4^-, whereas the D_{2h} structure was predicted to be the global minimum of neutral Au_4.[13] However, experimental vibrational data which provide structural information have not been available for Au_4 and Au_4^-. A partially resolved vibrational progression was obtained for the ground state PES band of Au_4^-,[7] but no analysis or vibrational frequency was reported.

The current experiment was performed using our newly developed velocity-map imaging (VMI) system equipped with a laser vaporization supersonic cluster source and a modified Wiley-McLaren time-of-flight mass spectrometer,[14] as described in a recent study on Au_2^-.[1] Briefly, vibrationally cold Au_n^- clusters were produced by laser vaporization of a gold disk target with a helium carrier gas seeded with 5% Ar. The Au_4^- cluster of interest was mass selected and then introduced into the detachment region of the collinear VMI system. The photodetached electrons were accelerated and focused onto a 75-mm diameter position-sensitive microchannel plate detector coupled with a phosphor screen. Images of photoelectrons were captured by a charge-coupled device (CCD) camera. The tunable detachment laser is a Continuum Sunlite optical parametric oscillator (OPO) system (222.5 nm–709 nm, linewidth <0.3 cm^{-1}). For the current study, photoelectron images were averaged from 50 000 to 500 000 laser shots, quadrant symmetrized, and inverse-Abel transformed to obtain velocity distributions. The reconstruction was performed by both the Basex[15] and pBasex[16] programs, which yielded similar results. The best resolution of the current VMI lens is 1.4 cm^{-1} calibrated by near threshold electrons of Bi^- and about 1% ($\Delta E/E$) for photoelectron kinetic energies higher than 1 eV.

Figure 1 shows the PE spectrum of Au_4^- at 355 nm (3.496 eV). A broad vibrational progression was observed with at least seven partially resolved vibrational peaks labeled as A–G. To obtain high resolution spectra, we tuned

a)E-mail: Lai-Sheng_Wang@brown.edu

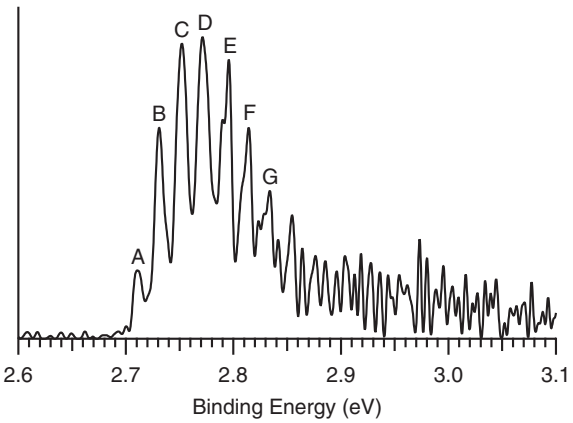

FIG. 1. Photoelectron spectrum of Au_4^- at 355 nm (3.496 eV).

the OPO to just above each vibrational peak. The PE images and the high resolution spectra are presented in Fig. 2, spanning the photon energy range from 456.54 nm (2.7158 eV) to 435.02 nm (2.8501 eV). The images presented have been transformed by pBasex[16] and the double arrow in Fig. 2(a) indicates the polarization of the detachment laser. All the spectra were taken under fairly cold experimental conditions[17] and no vibrational hot band was observed. Near threshold enhancement is observed, which is seen more clearly in Figs. 2(g) and 2(h). The high binding energy (low kinetic energy) part of each spectrum has the highest resolution. Just plotting this part of the spectrum would yield a so-called SEVI (slow-electron velocity-map imaging) spectrum, coined by the Neumark group.[4] Peak A represents the 0-0 detachment transition from the ground vibrational level of Au_4^- to that of Au_4 and defines the electron affinity (EA) of Au_4. Figure 2(a) yields a 6 cm^{-1} line width for peak A and an accurate EA of 2.7098 ± 0.0006 eV for Au_4. The positions of peaks B to G, given in Table S1 in the supplementary material,[18] are measured from Fig. 2(c) to 2(h), respectively. Peak D defines the VDE as 2.7728 ± 0.0006 eV. Fitting the Birge-Sponer plot for the vibrational spacing yields a fundamental vibrational frequency of $\omega_e = 171 \pm 7$ cm^{-1} and an anharmonicity $\omega_e\chi_e = \sim 0.5$ cm^{-1} for the main vibrational progression observed for Au_4.

The high resolution spectra in Fig. 2 reveal additional vibrational features, which have weak Franck-Condon factors. Associated with each main vibrational peak, there is a very weak feature about 17 cm^{-1} on the higher binding energy side. These features, labeled as b and c, are shown more clearly for peaks B and C in Figs. 2(c) and 2(d) (see the insets), respectively. The binding energies of these two peaks are also given in Table S1 in the supplementary material.[18] The intensities of these weak features are very low and are not clearly discernible in every spectrum. These weak features should correspond to a low frequency vibrational mode of Au_4.

In addition, weak signals are also observed in between the main vibrational peaks, which are discernible in Fig. 2(h) and shown more clearly in the 430.50 nm spectrum in Fig. S1 (labeled from a′ to f′) in the supplementary material.[18] However, this additional feature between peaks A and B (labeled as a′) is dramatically enhanced near the threshold at 454.87 nm, as shown in Fig. 2(b). The enhancement of peak a′ was observed within a 30 cm^{-1} photon energy range around 454.87 nm. It is separated from peak A by 97 cm^{-1} and should represent a third vibrational mode of Au_4. We also tried to observe similar threshold enhancement for the 97 cm^{-1} mode associated with the higher vibrational levels of the main progression, but did not observe any similar dramatic enhancement as that of peak a′ shown in Fig. 2(b). It seems that the threshold enhancement phenomenon is not simply a result of the Wigner threshold law.[19] Some other mechanisms, such as vibronic couplings or even shape resonances, may be at play.

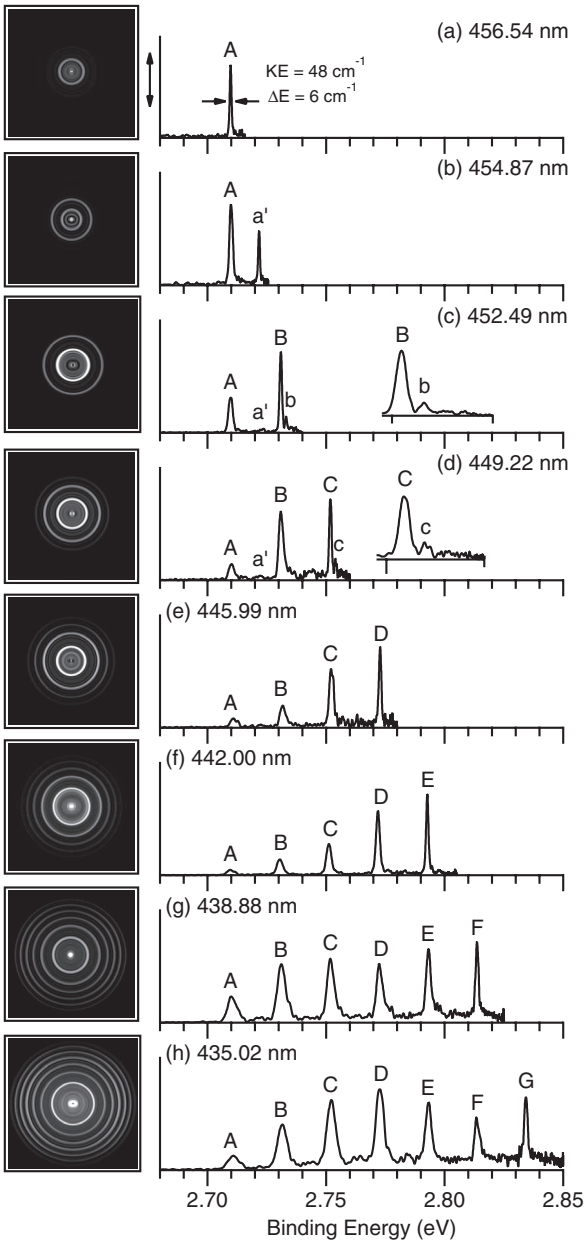

FIG. 2. Photoelectron images after the inverse-Abel transformation and spectra of Au_4^- at different detachment photon energies: (a) 456.54 nm (2.7158 eV), (b) 454.87 nm (2.7258 eV), (c) 452.49 nm (2.7400 eV), (d) 449.22 nm (2.7600 eV), (e) 445.99 nm (2.7800 eV), (f) 442.00 (2.8051) eV, (g) 438.88 nm (2.8250 eV), and (h) 435.02 nm (2.8501 eV). The double arrow in (a) indicates the laser polarization.

TABLE I. The vibrational modes and the calculated frequencies (unscaled) for the C_{2v} Y-shaped Au_4 in comparison with the experimental data.

Mode	Description	Calc. (cm^{-1})	Expt. (cm^{-1})[a]
ν_1 (a_1)	Breathing of Au_3	177	
ν_2 (a_1)	Au-Au stretching	147	171 (7)[b]
ν_3 (a_1)	Symmetric Au-Au_2 stretching	72	97 (7)
ν_4 (b_1)	Bending	31	
ν_5 (b_2)	Asymmetric Au-Au_2 stretching	74	
ν_6 (b_2)	Au wagging	14	17 (7)

[a]The number in the parentheses represents the uncertainty.
[b]Harmonic frequency (ω_e) from fitting to a Birge-Sponer plot. The anharmonicity ($\omega_e x_e$) is ~0.5 cm^{-1}.

We have also tried to obtain spectra of Au_4^- under hot source conditions, in order to obtain vibrational information for the anion, as shown in Fig. S1 in the supplementary material at two photon energies.[18] This was accomplished simply by performing experiments for clusters, which exited the nozzle early, i.e., with a short residence time inside the nozzle, as described previously.[20] The hot band observed in Fig. S1 in the supplementary material yields a vibrational frequency of 135 ± 15 cm^{-1} for Au_4^-, considerably lower than the 171 cm^{-1} frequency obtained for neutral Au_4.[18]

To assist with the assignments of the observed vibrational modes, we calculated the frequencies for both the C_{2v} Y-shaped Au_4 and the D_{2h} rhombus Au_4 using Gaussian 09 at the B3LYP/lanl2dz level.[21] The highest and lowest frequencies for the rhombus structures are 155 and 31 cm^{-1} (Fig. S2 in the supplementary material),[18] respectively. The latter is inconsistent with our observed lowest frequency of 17 cm^{-1}. This is in agreement with both previous ion mobility and PES experiments that have already confirmed the global minimum of Au_4^- to be the Y-shaped structure.[9,11] Table I compares the calculated frequencies of the C_{2v} structure with the experimental results. Even though the observed 171 cm^{-1} mode agrees well with the calculated frequency of the ν_1 mode, we think the observed main vibrational progression should be due to the ν_2 mode based on the nature of the orbital from which the electron is removed (Fig. 3(a)) and the nature of the normal modes (Fig. 3(b)). The singly occupied molecular orbital (SOMO) of Au_4^- shows an antibonding interaction between the Au_2 in the base of the Au_3 moiety (Fig. 3(a)). Thus, the ν_2 mode, which involves the Au–Au stretching, is expected to have the largest Franck-Condon activity. The ν_2 frequency is also expected to be significantly reduced in the anion relative to that in the neutral, in agreement with our experimental observation. Figure S3 in the supplementary material gives the calculated frequencies of the C_{2v} Au_4^-,[18] which shows that among all the modes the ν_2 mode has the largest frequency decrease of 40 cm^{-1} relative to the neutral, which is in excellent agreement with the experimental observation of a 36 cm^{-1} drop (171 cm^{-1} in Au_4 vs 135 cm^{-1} in Au_4^-). It should be noted that because photodetachment is a vertical process the D_{2h} Au_4 structure, which is predicted to be the most stable structure of the neutral,[13] is not accessible from photodetachment of the C_{2v} Au_4^-. Hence, the observed EA and vibrational frequencies are all pertained to the Y-shaped Au_4.

The observed 97 cm^{-1} mode is assigned to the ν_3 mode with a calculated frequency of 72 cm^{-1}. The ν_3 mode can be viewed as a symmetric Au–Au_2 stretching. The weak Franck-Condon activity is consistent with the nature of the SOMO of Au_4^-. The 17 cm^{-1} mode must be due to the ν_6 (b_2) mode, which involves the wagging motion of the dangling Au atom relative to the Au_3 moiety (Fig. 3(b)). This mode is not totally symmetric and is not allowed if both the anion and neutral have C_{2v} symmetry. Even though the Franck-Condon factor of this mode is extremely small, its observation suggests that the bonding of the dangling Au atom with the Au_3 moiety is weak and the potential energy curve for the Au wagging is probably rather flat.

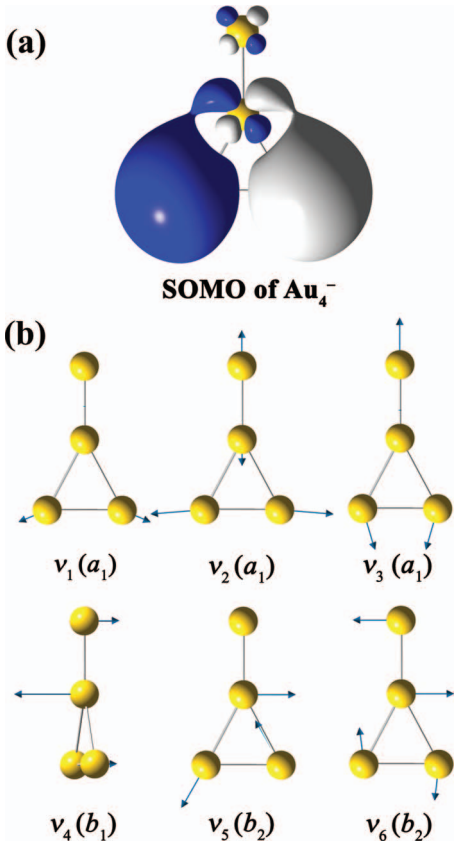

FIG. 3. (a) The singly occupied molecular orbital (SOMO) of the global minimum Y-shaped Au_4^- (C_{2v}, $^1A_1$). (b) The normal modes of vibration of the Y-shaped Au_4.

The angular distributions from PE imaging also provide important electronic structure information. For single photon detachment, the angular distribution is given by[22,23]

$$d\sigma/d\Omega = \sigma_{tot}/4\pi[1 + \beta(3/2\cos^2\theta - 1/2)], \quad (1)$$

where θ is the angle between the direction of the photoelectrons and the polarization vector of the detachment photon. The anisotropy parameter β lies between −1 and 2, and provides information about the orbital angular momentum (l) of the ejected photoelectrons: $\beta = 0$ for $l = 0$ (s-wave), $\beta = 2$ for $l = 1$ (p-wave), and $\beta = -1$ for $l = 0$ and 2 with equal amplitude and phase ($s + d$ wave). Fitting Eq. (1) to the photoelectron intensity versus angle at a given radius of the PE images yields the anisotropy parameter β for a given vibrational peak of Au_4.

For all the vibrational peaks in the PE images of Au_4^-, the photoelectron intensity is more intense in the direction perpendicular to the laser polarization, corresponding to the $s + d$ waves. This observation suggests that the electrons are detached from a p-type orbital, which is consistent with the shape of the SOMO of Au_4^- (Fig. 3(a)). Figure S4a in the supplementary material presents the β values obtained for the vibrational peaks of the ν_2 mode for the PE image taken at 435.02 nm (Fig. 2(h)), while Fig. S4b in the supplementary material shows the dependence of the β parameter of the 0-0 transition on the photoelectron kinetic energies.[18] Both plots show a similar trend: β approaches zero with decreasing kinetic energies. This is a result of the threshold law. When the photoelectron is detached from a p-type orbital, the s-wave ($l = 0$) dominates near threshold, giving rise to more isotropic angular distributions. With increasing kinetic energies, the d-wave contributes more and interference between the s- and d-wave results in the nearly perpendicular angular distributions.

The current study demonstrates that high resolution PE imaging will provide both electronic and vibrational information for size-selected clusters, which will be valuable for cluster structure determination. Because of the different selection rules, high resolution PE imaging will be complementary to infrared spectroscopy in providing vibrational information for size-selected clusters. In fact, the ability to observe low frequency vibrations from high resolution PE imaging may even rival infrared spectroscopy.

This research was supported by the National Science Foundation (NSF) (CHE-1049717). I.L. thanks the Basque Government for a postdoctoral fellowship.

[1]I. León, Z. Yang, and L. S. Wang, J. Chem. Phys. **138**, 184304 (2013).
[2]D. W. Chandler and P. L. Houston, J. Chem. Phys. **87**, 1445 (1987).
[3]A. T. J. B. Eppink and D. H. Parker, Rev. Sci. Instrum. **68**, 3477 (1997).
[4]D. M. Neumark, J. Phys. Chem. A **112**, 13287 (2008).
[5]J. Ho, K. Ervin, and W. C. Lineberger, J. Chem. Phys. **93**, 6987 (1990).
[6]H. Handschuh, G. Ganteför, P. S. Bechthold, and W. Eberhardt, J. Chem. Phys. **100**, 7093 (1994).
[7]H. Handschuh, G. Ganteför, and W. Eberhardt, Rev. Sci. Instrum. **66**, 3838 (1995).
[8]H. Grönbeck and W. Andreoni, Chem. Phys. **262**, 1 (2000).
[9]F. Furche, R. Ahlrichs, P. Weis, C. Jacob, S. Gilb, T. Bierweiler, and M. M. Kappes, J. Chem. Phys. **117**, 6982 (2002).
[10]J. L. Wang, G. H. Wang, and J. J. Zhao, Phys. Rev. B **66**, 035418 (2002).
[11]H. Häkkinen, B. Yoon, U. Landman, X. Li, H. J. Zhai, and L. S. Wang, J. Phys. Chem. A **107**, 6168 (2003).
[12]G. P. Li and I. P. Hamilton, Chem. Phys. Lett. **420**, 474 (2006).
[13]Y. Gao, Y. Zhao, and X. C. Zeng, J. Theor. Comput. Chem. **9**, 1 (2010).
[14]L. S. Wang, H. S. Cheng, and J. W. Fan, J. Chem. Phys. **102**, 9480 (1995).
[15]V. Dribinski, A. Ossadtchi, V. A. Mandelshtam, and H. Reisler, Rev. Sci. Instrum. **73**, 2634 (2002).
[16]G. A. Garcia, L. Nahon, and I. Powis, Rev. Sci. Instrum. **75**, 4989 (2004).
[17]W. Huang and L. S. Wang, Phys. Rev. Lett. **102**, 153401 (2009).
[18]See supplementary material at http://dx.doi.org/10.1063/1.4813503 for the listing of the binding energies of all the observed transitions and their assignments; spectra taken at 456.55 and 430.50 nm under hot source conditions; and calculated vibrational modes and frequencies for the D_{2h} Au_4 and the C_{2v} Au_4^-.
[19]E. P. Wigner, Phys. Rev. **73**, 1002 (1948).
[20]J. Akola, M. Manninen, H. Hakkinen, U. Landman, X. Li, and L. S. Wang, Phys. Rev. B **60**, R11297 (1999).
[21]P. J. Hay and W. R. Wadt, J. Chem. Phys. **82**, 299 (1985).
[22]J. Cooper and R. N. Zare, J. Chem. Phys. **48**, 942 (1968).
[23]K. L. Reid, Annu. Rev. Phys. Chem. **54**, 397 (2003).